J. Plasma Fusion Res. SERIES, Vol. 6 (2004) 349–352

Low *m*/*n* Mode Behavior of MHD Plasma in LHD

MIURA Hideaki and HAYASHI Takaya
National Institute for Fusion Science, Toki 509-5292, Japan
(Received: 9 December 2003 / Accepted: 22 January 2004)

Abstract

Behaviors of low poloidal (m) and toroidal (n) Fourier modes in the Large Helical Device (LHD) are investigated by means of direct numerical simulations (DNS) of fully three-dimensional, nonlinear and compressible magnetohydrodynamics (MHD) equations. Starting from an ideal equilibrium with the position of vacuum magnetic axis $R_{ax} = 3.6\ m$ and $\beta_0 = 4\%$ finite pressure, a $m/n = 2/1$ mode grows in the DNS. Fluid motions on poloidal sections are governed by the two pairs of anti-parallel vortex pairs associated with the $m/n = 2/1$ modes. The vortex pairs transport plasma pressure from the core to edge region and bring about large pressure deformations. It is also shown that the toroidal part in the kinetic energy and the enstrophy are comparable to the poloidal parts of them. The numerical results demonstrate importance of investigating three-dimensional behaviors of MHD plasmas in LHD.

Keywords:

magnetohydrodynamic, direct numerical simulation, $m/n = 2/1$ mode, vortex pair

1. Introduction

Understanding MHD behaviors is one of the most important subjects to understand physics of plasma confinment in LHD. MHD fluids in LHD are exposed to various physical mechanism such as the steep pressure gradient and the curvature effects of the magnetic field lines. These mechanism have been expected to cause MHD instabilities when so-called inward-shifted magnetic field configuration is adopted. However, recent experiments with $R_{ax} = 3.6\ m$ (inward-shifted) vacuum magnetic axis revealed that the plasma was confined very well in spite of the Mercier-unstable nature of the magnetic field [1]. It is reported in the article that, even though an $m/n = 2/1$ MHD activity appeared when the averaged beta $\langle\beta\rangle$ stayed for $1\% < \langle\beta\rangle < 2.2\%$, it did not destroy the confinment. It suggests that there should be some stabilization mechanism which suppress instabilities.

In order to investigate MHD behaviors in full three-dimensional (3D) geometry of LHD, direct numerical simulations (DNS) of MHD equations is one of the best approaches. In this article, we conduct DNS of full 3D, compressible, dissipative and nonlinear MHD equations which start from an equillibrium with $R_{ax} = 3.6\ m$ and report on low-n behaviors of the MHD plasmas. Though the full-torus evolution of the MHD plasma with the same initial equilibrium is partially reported in the previous work [2], only a few aspects of the numerical results are described and detailed fluid motions are not presented there. In this article, the simulation results are reported with special attention to fluid motions.

2. Direct numerical simulations

The MHD equations are described in the helical-toroidal coordinate system. Detailed information about our numerical code is reported in Ref. 3. The number of grid points is 97×97 on poloidal sections and 640 in the toroidal direction. The MHD fluid is assumed to obey to the equation of an ideal gas with the ratio of specific heats $\gamma = 1.4$. The non-dimensional parameters of the MHD equations are the heat conductivity $\kappa = 1 \times 10^{-6}$, the resistivity $\mu = 1 \times 10^{-5}$ and the viscosity $\nu = 2 \times 10^{-3}$.

The initial condition is provided by making use of the HINT code [4]. The HINT computation gives a 3D MHD equilibrium in a helical system. In our previous work, an MHD equilibrium in the LHD system with $R_{ax} = 3.6\ m$ and $\beta_0 = 4\%$ was obtained [5]. Starting from the equilibrium, the plasma is dominated by the resistive ballooning instability if the system is under the stellarator (half-pitch) symmetry. Here we investigate behaviors of the MHD plasma starting from the same equilibrium but without the half-pitch symmetry.

In Fig. 1, the time evolution of the kinetic energy $\langle k\rangle = \langle\rho|\boldsymbol{v}|^2/2\rangle$ is shown, where $\boldsymbol{v} = (v^1, v^2, v^3)$ is the velocity vector and the brackets $\langle\cdot\rangle$ represent the volume average. The kinetic energy begins to grow rapidly at $t \simeq 200\ \tau_A$. At $t \simeq 200\ \tau_A$, we observe ballooning-like fluctuations on horizontally-elongated poloidal sections. In Fig. 2, the pressure profile on a horizontally-elongated poloidal section is shown at $t = 180$,

Corresponding author's e-mail: miura@toki.theory.nifs.ac.jp

280, 350, 500, 600 and 700 τ_A. The pressure is higher for darker shades. The two thick solid ellipses represent magnetic surfaces with the rotational transform $\iota/2\pi = 0.5$ and 0.66 at the initial time, respectively. Thin lines represent streamlines depicted with the poloidal components of the velocity vector $\boldsymbol{v}_{pol} = (v^1, v^2)$. As time evolves from the initial state to

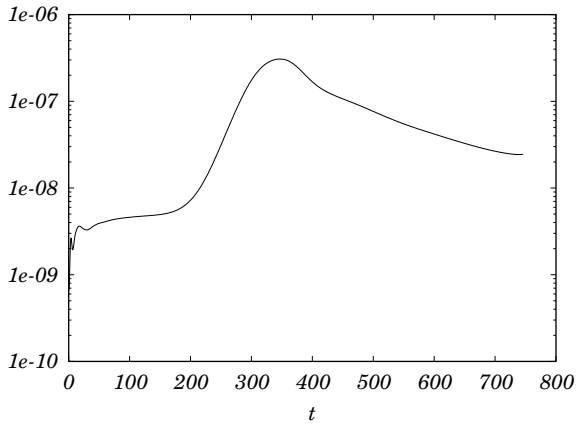

Fig. 1 Time evolution of the kinetic energy.

t = 180, 280 and 350 τ_A, the two anti-parallel vortex pairs associated with the m/n = 2/1 mode are strongly excited. Because of the mutual advection of the anti-parallel vortex pairs, the high-pressure regions are divided into two groups, advected and stretched toward the edge region. Consequently, two mushroom-like structures are formed on poloidal sections. The formation of the mushroom structures leads to generation of the secondary vortex structures, as are observed at t = 500 τ_A. After t = 500 τ_A, the vortices become weaker and the mushroom structures become ambiguous. The plasma finaly forms a broad pressure profile at the core and relaxes to inactive state t = 700 τ_A.

Now we should pay attentions to the point that streamlines in Fig. 2 have sinks or sources. Though streamlines do not represent strength of streams directly, the dense convergent streamlines suggest that there are strong sinks or sources there. The sinks or sources of the two-dimensional stremlines come either from three-dimensionality or from compressibility of the velocity field. In Fig. 3(a), the mean kinetic energy $\langle k \rangle = \langle \rho |\boldsymbol{v}|^2/2 \rangle$ is compared to its two-dimensional contribution $\langle k_{pol} \rangle = \langle \rho |\boldsymbol{v}_{pol}|^2/2 \rangle$. We find that $\langle k_{pol} \rangle$ (dotted line) is as large as one-half of $\langle k \rangle$ (solid line) at most. It implies that the toroidal component of the velocity

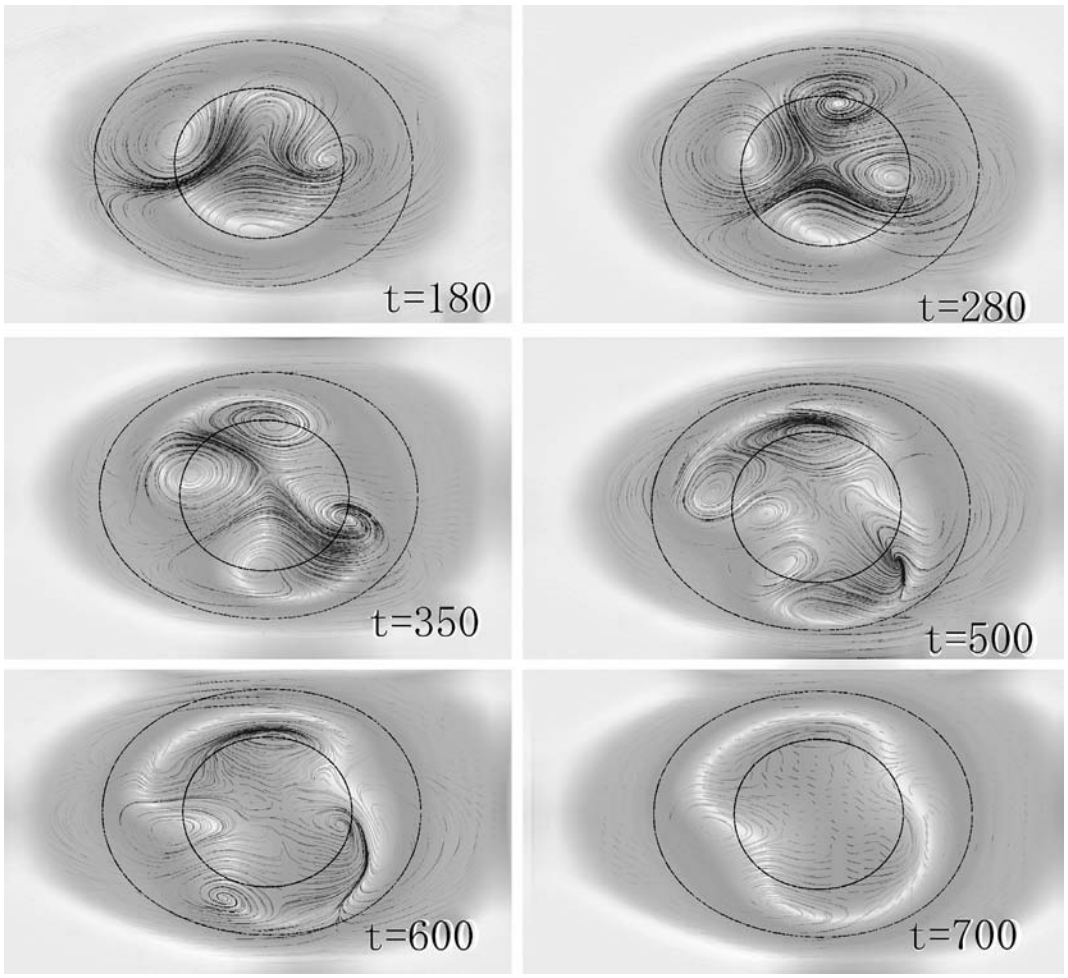

Fig. 2 Pressure and streamlines on a poloidal section at a few time snapshots.

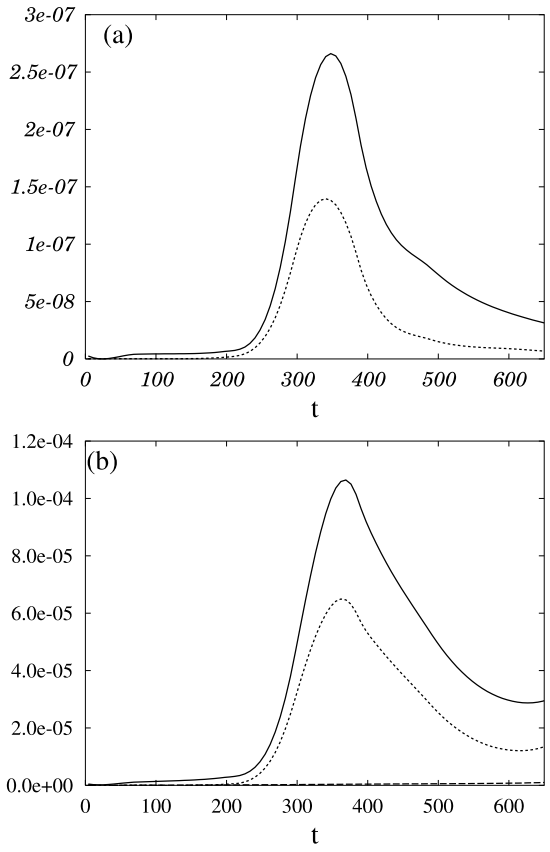

Fig. 3 (a) Time evolutions of mean values of the three-dimensional velocity magnitude $\langle k \rangle$ (solid line) and the two-dimensional magnitude $\langle k_{pol} \rangle$ (dashed line). (b) Time evolutions of the enstrophy $\langle Q \rangle$ (solid line), its toroidal component $\langle Q_{tol} \rangle$ (dashed line) and the mean squared dilatation $\langle (\nabla \cdot \boldsymbol{v})^2 \rangle$.

v^3 occupies a significant part of the kinetic energy. In Fig. 3(b), the mean enstrophy $\langle Q \rangle = \langle |\boldsymbol{\omega}|^2/2 \rangle$ is compared to the toroidal component of the vorticity $\langle Q_{tol} \rangle = \langle \omega_3 \omega^3/2 \rangle$, where $\boldsymbol{\omega} = \nabla \times \boldsymbol{v}$ is the vorticity and ω_3 (ω^3) is covariant (contravariant) component (calculated by v^1 and v^2) of the vorticity vector. We find that $\langle Q_{tol} \rangle$ occupies 2/3 of $\langle Q \rangle$ at most. These two comparisons indicate that the fluid motions are fully three-dimensional and that the toroidal motions of the plasma is as important as those on poloidal sections. In Fig. 3(b), the mean squared dilatation $\langle (\nabla \cdot \boldsymbol{v})^2 \rangle$ is compared to $\langle Q \rangle$ and $\langle Q_{tol} \rangle$. It is clear that $\langle (\nabla \cdot \boldsymbol{v})^2 \rangle$ (dashed line) is quite smaller than the other two quantities. It indicates that direct contributions of compressibility to the fluid motions are very small, though there can be some indirect compressibility effectsto fluid motions. (Note that, in neutral fluid turbulence, small compressibility can cause significant changes in vortex structures [5].)

Three-dimensional natures of fluid motions are more clearly seen in isosurfaces of the pressure p in Fig. 4(a) and ω^3 in Fig. 4(b). A clear m/n = 2/1 structure is observed in Fig. 4(a). However, the isosurfaces are strongly distorted near the horizontally-elongated cross-sections. It suggests that the structure is not very simple but consists of some other

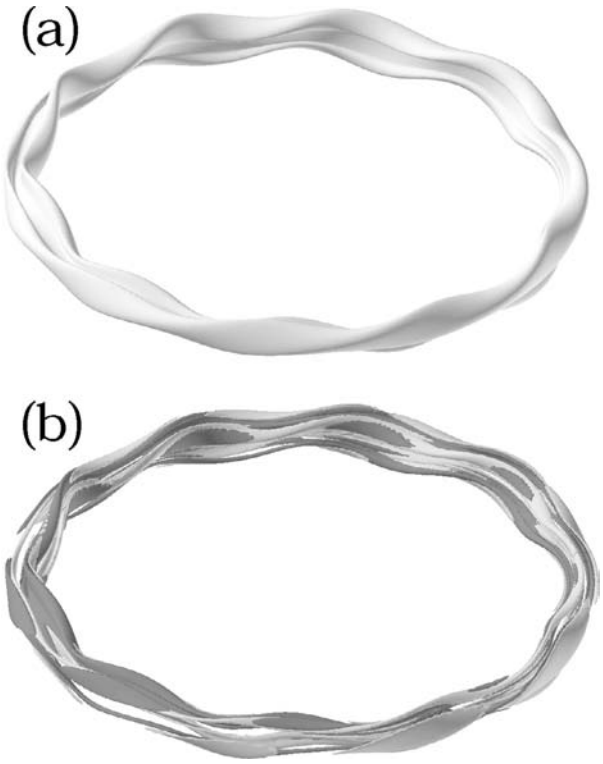

Fig. 4 (a) Isosurface of the pressure. (b) Isosurfaces of the toroidal vorticity ω_{tol}. Dark and light shades represent positive and negative signs of ω_{tol}, respectively.

(typically n = 10) modes, although m/n = 2/1 is the most dominant mode. The three-dimensional structures of the toroidal vorticity ω_{tol} in Fig. 4(b) are more complicated than those of p. We find that dark- and light-shaded isosurfaces (for positive and negative ω^3, respectively) come to the inner-side of the torus alternately ten times. It means that n = 10 modes have finite amplitudes. It is quite reasonable to consider that the growth of multiple modes is one of the mechanism which brings about (nonlinear) saturation of the kinetic energy growth in Fig. 1.

3. Summary

We have conducted fully toroidal DNS of MHD plasma in LHD and observed growth of m/n = 2/1 modes. The m/n = 2/1 anti-parallel vortex pairs transport plasma pressure from the core to edge region, and are relaxed to an inactive state. Though toroidal motions have not been investigated very much, our numerical results suggest that toroidal motions are as important as poloidal motions (vortex structures) for pressure transports in MHD. Detailed analysis on growth, saturation and relaxation of m/n = 2/1 modes and pressure transport associated with the m/n = 2/1 mode will be reported elsewhere.

References

[1] O. Motojima *et al.*, Nucl. Fusion **43** 1674, (2003).
[2] H. Harafuji *et al.*, J. Comp. Phys. **81** 169, (1989).
[3] H. Miura *et al.*, J. Plasma Fusion Res. SERIES **5** 495,

(2002).

[4] H. Miura *et al.*, J. Plasma Fusion Res. SERIES **4** 476, (2001).

[5] H. Miura, *in Proc. IUTAM Symposium on Reynolds Number Scaling in Turbulent Flow* (ed. by A.L. Smits), Kluwer Academic Press 237, (2003).